

## REVIEW

# Natural source of carbon dots from part of a plant and its applications: a review

 Nurul Amalia Humaera | Ahmad Nurul Fahri | Bidayatul Armynah | Dahlang Tahir 

Department of Physics, Hasanuddin University, Makassar, Indonesia

**Correspondence**
 Dahlang Tahir, Department of Physics, Hasanuddin University, Makassar 90245, Indonesia.  
 Email: dtahir@fmipa.unhas.ac.id
**Funding information**

Indonesian Government (Kemenristek/BRIN), Grant/Award Number: 1516/UN4.22/PT.01.03/2021

**Abstract**

Carbon dots (CDs) are carbon nanoparticles with a size of less than 10 nm, and are synthesized from various sources; they have been of great interest to scientists worldwide due to their unique optical, electrical, and chemical properties. Sources of carbon are inexpensive and can be classified as a renewable natural resources. Many researchers use CDs because of their low toxicity, better water solubility, high biocompatibility, and stable photoluminescence. The simple methods for producing CDs are hydrothermal and use inexpensive equipment, have low energy consumption, simple manipulation, and one-step preparation. Since the discovery of CDs, researchers have used them in various applications such as sensing, bioimaging, drug delivery, and catalysis. In this review, CDs synthesized from natural resources such as samples from herbs, roots, leaves, flowers, and fruit and some applications are described. This review provides a summary of carbon dots that is expected to provide further information for development of new CDs.

**KEYWORDS**

biomedical applications, carbon dots (CDs), photocatalyst, source of carbon

## 1 | INTRODUCTION

CDs were discovered accidentally during the separation and purification of single-walled carbon nanotubes, and have a carbon size of less than 10 nm.<sup>[1]</sup> CDs were also called carbon quantum dots or also carbon nanoparticles (CNPs) during their first synthesis in 2004.<sup>[2]</sup> Scientists worldwide have studied CDs due to their excellent photostability, favourable biocompatibility, low toxicity, and good water solubility.<sup>[3]</sup> CDs are generally pseudonanoparticles that are amorphous and nanocrystalline and always consist of sp<sup>2</sup>/sp<sup>3</sup> carbon, oxygen/nitrogen-based groups, and postmodified chemical groups.<sup>[4]</sup>

The synthesis of CDs can be carried out using simple methods and various techniques such as microwave-based methods, laser ablation, electrochemical oxidation, and hydrothermal treatment. However, hydrothermal synthesis is considered one of the simplest methods for producing CDs as it needs inexpensive equipment, and has low energy consumption, simple manipulation, and a one-step preparation.<sup>[5]</sup> In particular, hydrothermal synthesis can produce CDs self-passively without posttreatment.<sup>[1]</sup>

It has been reported<sup>6</sup> that the chemiluminescence (CL) properties of CDs are through the generation of electromagnetic radiation from chemical reactions. CL is a promising technique with increased reliability, fast response, efficient instrumentation, and simple operation.<sup>[6]</sup> In 2017, Lin et al. reported the effect of carbon nanodots on the H<sub>2</sub>O<sub>2</sub>-NaHSO<sub>3</sub> system, and batch CL experiments were used to evaluate the effect of various injection solutions. This study showed that injection of a H<sub>2</sub>O<sub>2</sub> solution into NaHSO<sub>3</sub>-carbon nanodots solution generated the strongest CL emission giving an approximately 60-fold increase in CL intensity and reached the maximum value rapidly.<sup>[7]</sup>

In 2016, Shah et al. demonstrated the enhancement of KIO<sub>4</sub>-H<sub>2</sub>O<sub>2</sub> CL using N-CDs to determine pyrogallol and gallic acid. N-CDs dramatically boosted their CL intensity in the KIO<sub>4</sub>-H<sub>2</sub>O<sub>2</sub> system due to surface energy traps.<sup>[8]</sup> Enhanced CL was used to determine pyrogallol and gallic acid over the range 1.0 × 10<sup>-4</sup> to 1.0 × 10<sup>-7</sup> M with a limit of detection of 4.6 × 10<sup>-8</sup> to 6.1 × 10<sup>-8</sup> M.<sup>[8]</sup>

CDs prepared using hydrothermal methods have abundant hydroxyl, carboxyl, or epoxy groups that are produced through

oxidation of the raw material (bulk carbon material) or partially carbonized organic carbohydrates that produce oligosaccharide and aliphatic chains, which are condensed on the surface of the CDs. Carbon nanostructured materials, nitrogen substitution, or substitutional N-doping, have been powerful methods to tailor the properties of carbon nanostructured materials and render their potential use for various applications. However, most nitrogen atoms induced on particle surfaces have a low N/C atomic ratio, and most have low content of less than 10%. In 2017, Zheng et al. successfully for first time synthesized a new nitrogen quantum dots with a very high percentage of nitrogen of approximately 57%. The N-dots exhibited unique optical properties with a 400-fold increase in the ultraweak chemiluminescent reaction of  $\text{NaIO}_4\text{-H}_2\text{O}_2$ .<sup>[9]</sup>

Photoluminescence (PL) is one of the most attractive features of CDs due to quenching via electrons from acceptors or donors, promising for manipulation of photoinduced electron transfer. CDs have strong PL emission in the visible spectral range and are easy to synthesize and surface modify, with excellent water solubility, and low toxicity. Therefore, CDs have great potential for biomedical applications in biosensing, bioimaging, and drug delivery.<sup>[10]</sup> Bioimaging applications of luminous nanomaterials use a new class of NIR-II gold nanoclusters with protein biolabels for *in vivo* tumour-targeted imaging,<sup>[11]</sup> observing antimicrobial processes with traceable gold nanoclusters,<sup>[12]</sup> and atomic-precision gold clusters for NIR-II imaging.<sup>[13]</sup>

The synthesis of CDs can be carried out using various carbon sources or precursors. Natural materials are one of the most popular and readily available materials compared with the chemicals needed as precursors to produce CDs and are beneficial for large-scale production and industrial applications. Natural renewable sources generate green CDs that have outstanding properties such as low cost, high availability, high yield, high biocompatibility, and high renewable capability.<sup>[14]</sup> Various natural materials as sources of CDs are apple,<sup>[15]</sup> jackfruit,<sup>[16]</sup> cabbage,<sup>[17]</sup> orange,<sup>[18]</sup> banana,<sup>[19]</sup> oolong tea,<sup>[20]</sup> pear,<sup>[21]</sup> jujubes,<sup>[22]</sup> betel leaf,<sup>[23]</sup> guava leaf,<sup>[24]</sup> bamboo leaf,<sup>[25]</sup> etc. Although natural ingredients have been widely used, there have still some weaknesses that have not been fully resolved.

Most synthesized methods are still at the development stage and generate problems of stability and aggregation of nanoparticles, control of crystal growth, morphology, size, and size distribution. However, in recent years, the green synthesis of nanoparticles has become a major interest for researchers as a way to produce CDs from plants due to their high stability and faster synthesis rate compared with that of microorganisms.<sup>[26]</sup>

Green chemistry methods for synthesis has been one of the key technologies for innovation with principles such as waste prevention, economy, less hazardous synthesis, and design of safer chemicals, safer solvents and auxiliaries, plus energy efficiency, renewable feedstock, reducing derivatives, using catalysts with better selectivity compared with using stoichiometric reagents, design of degradable products, and use of inherently safer chemistry aimed at accident prevention.<sup>[27]</sup> Applications of CDs are broad and cover a wide variety of

fields including sensing,<sup>[4]</sup> imaging,<sup>[2]</sup> drug delivery,<sup>[28]</sup> and catalysis.<sup>[29]</sup>

This paper provides a nonexhaustive but comprehensive review of CD material research. It covers the sources of carbon such as bulbs, flower, leaf, and fruits (Section 2) and its applications: sensing, bioimaging, drug delivery and catalysis (Section 3). In particular, sensing, drug delivery, and photocatalyst mechanism of CDs are discussed.

## 2 | SOURCE OF CARBON

Carbon sources in the form of natural materials are abundant in nature for example as plants. Many researchers have used parts of plants as carbon sources, as presented in Table 1. Selected plant parts are bulbs, flowers, leaves, and fruits.

### 2.1 | Bulbs

Bulbs are the part of the plant that lies in the soil, or more precisely the roots of plants. Researchers have used these bulbs as a natural carbon source through hydrothermal treatment of plants such as rose-heart radish, carrots, and sweet potato. In 2017, Liu et al. used rose-heart radish as a carbon precursor and doped nitrogen to synthesize green N-CDs using hydrothermal treatment at 180°C for 3 h; the resulting CD size was within the range 1.2–6.0 nm with a 13.6% quantum yield.<sup>[32]</sup> In 2018, D'Souza et al. reported *Daucus carota* subsp. *sativus* (carrot) roots as a carbon source for fluorescent CDs using hydrothermal treatment. Carrot roots are important plant parts that contain carbohydrates, carotenoids, polyphenols, and dietary fibres.<sup>[28]</sup> Fluorescent CDs involve the carbonization of chemical compounds through hydrolysis, dehydration, and decomposition giving the resulting small size of approximately 2.3 nm with a quantum yield of 7.6% (Figure 1).

CDs were synthesized from sweet potato by crushing with water in a blender at high-speed and then heating at 80°C for 3.5 h to break the cell wall. Using this method, the polysaccharides from sweet potato were of high yield, therefore making sweet potato a carbon-based precursor.<sup>[1]</sup> In 2017, Shen et al. described a facile synthesis method using sweet potato for fluorescent CDs with small size ranges from 2.5 to 5.5 nm and quantum yield of 8.64%.<sup>[1]</sup>

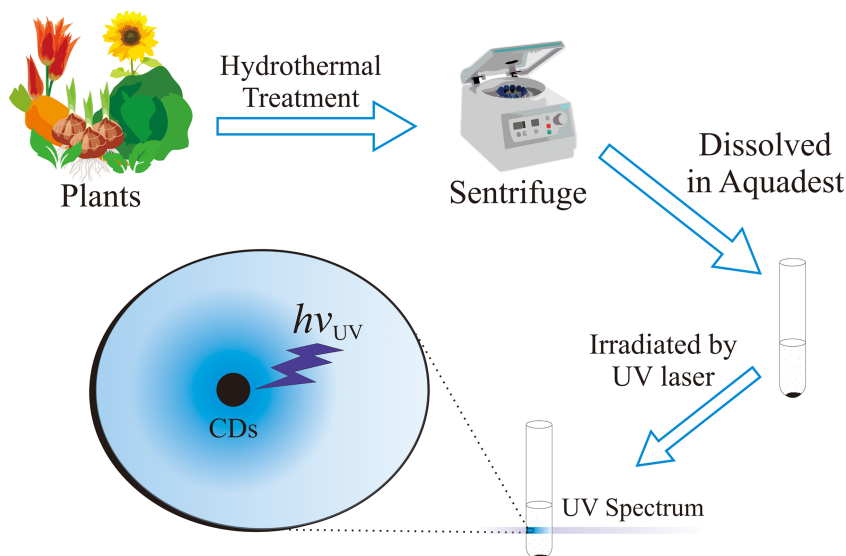
Chen et al. in 2015, reported a facile synthesis using garlic as a carbon precursor for N, S, and CDs with good water solubility, strong fluorescence, and upconversion of fluorescence without any further modification. N, S, and CDs had an average size for the monodisperse of approximately 3.6 nm with a quantum yield of 13%.<sup>[3]</sup> In addition, in 2015, Zhao et al. used garlic for green synthesis of bifunctional fluorescent CDs,<sup>[33]</sup> and Hu et al. synthesized S and N co-doped CDs from water chestnut and onion.<sup>[34]</sup> Another study on bulbs as a carbon source used potato scratch<sup>[35]</sup> and fresh potato.<sup>[5]</sup>

TABLE 1 Carbon sources and applications of CDs

Carbon source	CD size (nm)	Application	Ref
<i>Daucus carota</i> subsp. <i>sativus</i> (carrot)	2.3	Drug delivery	[28]
Potato	11	Sensing	[5]
Garlic	3.6	Sensing and imaging	[3]
Groundnut	2–8	Sensing and imaging	[30]
Potato	4.5	Optical devices	[31]
Rose-heart radish	1.2–6.0	Sensing and imaging	[32]
Sweet potato	2.5–5.5	Sensing and imaging	[1]
Garlic	11	Imaging	[33]
Water chestnut and onion	2–4	Imaging	[34]
<i>Abelmoschus manihot</i> (Linn.)	9	Imaging	[35]
<i>Magnolia liliiflora</i>	5	Sensing and imaging	[36]
<i>Syringa obtata</i> Lindl.	1–8	Sensing and imaging	[37]
Wheat bran	4.9	Drug delivery	[38]
<i>Nigella sativa</i>	2–6	Sensing	[39]
Broccoli	2–6	Sensing	[40]
Linseed	4–8	Sensing and imaging	[41]
Coriander	1.5–2.98	Sensing and imaging	[42]
Purple perilla	2.8	Sensing	[43]
Waste tea	10	Sensing	[44]
Tulsi leaves	5	Sensing and imaging	[45]
<i>Prosopis juliflora</i> leaves	5.8	Sensing	[46]
Betel leaves	3–7	Sensing	[23]
Bamboo leaves	11	Catalyst	[25]
Bamboo leaves	3.6	Sensing	[47]
Oolong tea	1.7–5.0	Sensing and imaging	[20]
<i>Ocimum sanctum</i>	3	Sensing and imaging	[48]
<i>Boswellia ovalifoliolata</i>	4.16 ± 0.22	Sensing	[49]
<i>Allium fistulosum</i>	4.22	Imaging	[2]
<i>Hibiscus sabdariffa</i>	4.85–7.78	Sensing and imaging	[50]
<i>Lawsonia inermis</i> (Henna)	3–7	Sensing	[51]
Cabbage	2–6	Imaging	[17]
Hongcaitai	1.6–2.3	Sensing and imaging	[52]
Spinach	3	Sensing	[53]
Enokitake mushroom	4	Sensing and imaging	[54]
Aloe	5	Sensing	[55]
<i>Sargassum fluitans</i>	2–8	Sensing	[56]
<i>Thymus vulgaris</i> L.		Sensing and imaging	[57]
Mulberry leaves	2–4	Drug delivery	[58]
<i>Actinidia deliciosa</i> ( <i>A. deliciosa</i> ) fruit	3.59	Imaging	[59]
Apple	1.5–6.5	Imaging	[15]
Banana	1.27	Sensing	[19]
<i>Chionanthus retusus</i> fruit	3–7	Sensing and imaging	[60]
Pomelo ( <i>Citrus maxima</i> or <i>Citrus grandis</i> )	3	Catalytic	[29]
Date kernel	2.5	Imaging	[61]
Gardenia	2.1	Sensing	[62]
Ginkgo fruits	3.81	Sensing	[63]

TABLE 1 (Continued)

Carbon source	CD size (nm)	Application	Ref
<i>H. undatus</i>	2.86	Imaging and catalytic	[64]
Jackfruit	5.4	Sensing	[16]
<i>Lantana camara</i> berries	3–8	Sensing and imaging	[65]
Lemon	4–5	Sensing	[66]
<i>Lycii fructus</i>	2–5	Sensing and imaging	[67]
Orange	1.5–4.5	Imaging	[18]
Orange	0.5–3.0	Sensing	[68]
Papaya	3.4–10.8	Sensing	[69]
<i>Phyllanthus acidus</i>	3.5–5.5	Sensing and imaging	[70]
<i>Prunus cerasifera</i>	3–5	Sensing and imaging	[71]
<i>Pyrus pyrifolia</i>	1–3.5	Sensing	[72]
Seville orange	4–6	Sensing	[73]
Strawberry	5.2	Sensing	[74]
Unripe peach	8	Imaging	[75]
Watermelon	3–7	Sensing and imaging	[76]
Red lentils	4–10	Sensing	[77]
<i>Carica papaya</i>	1.5–5.5	Imaging	[78]
Jujubes	3.12	Sensing	[22]
Pear	10	Sensing	[21]
<i>Phyllanthus emblica</i>	1–10	Catalytic	[79]
<i>Prunus mume</i>	9	Imaging	[80]
Walnut	12	Imaging	[81]
Grape peel	1.5–3	Sensing	[82]
Orange peel	2–7	Catalytic	[83]
Lemon peel	1–3	Sensing and catalytic	[84]
Areca nut husk	4–5	Optical devices	[85]
<i>Sterculia lychnophora</i>	5	Sensing	[86]
Winter melon	4.5–5.2	Imaging	[87]
Black sesame seeds	7.6	Sensing	[88]



**FIGURE 1** Schematic illustration using plants as a carbon source for CDs via the hydrothermal method<sup>[28,35,42]</sup>

## 2.2 | Flower

Several studies have been carried out using flowers as well as bulbs as a source of carbon, for example for *Syringa obtata* Lindl, *Magnolia liliiflora* and *Abelmoschus manihot* (Linn.). In 2018, Diao et al. studied fluorescent CDs with tunable emission using *Syringa oblata* Lindl for synthesis of blue and green fluorescent CDs (B-CDs and G-CDs). B-CDs were obtained from hydrothermal treatment at 200°C for 4 h and G-CDs were added to sodium hydroxide (NaOH) in the precursor solution. B-CDs showed a size distribution range from 1.0 to 5.0 nm, while G-CDs ranged from 2.0 to 8.0 nm. In addition, B-CDs exhibited a higher quantum yield of 12.4% compared with that of G-CDs of only 6.5%.<sup>[37]</sup>

In 2018, Atchudan et al. synthesized N-CDs from *Magnolia liliiflora* as a carbon precursor that had many phyto-constituents: essential oil and volatile components. It was useful for the formation of carbon-structured materials with an average size of 4 ± 1 nm and quantum yield of 11%.<sup>[36]</sup> In 2019, Wan et al. synthesized CDs using flowers of *Abelmoschus manihot* (Linn.), which exhibited strong blue emission with a fluorescence quantum yield of 30.8%.<sup>[35]</sup> Other studies also used flowers for example from linseed,<sup>[41]</sup> broccoli<sup>[40]</sup> and *Nigella sativa* seeds as a carbon source.<sup>[39]</sup>

## 2.3 | Leaf

Leaves are generally green in colour, grow from twigs, and function to trap energy from sunlight for photosynthesis. In 2014, Liu et al. reported bamboo leaves as a carbon source using a green hydrothermal method for high quantum yield carbon quantum dots (CQDs). These CQDs were modified with branched polyethyleneimine (BPEI) as a coating by electrostatic adsorption to give a particle size of approximately 3.4–4.2 nm and quantum yield of 7.1%.<sup>[47]</sup> Similar results were reported in 2020 by Yang et al. using bamboo leaves for green synthesis of fluorescent CDs.<sup>[25]</sup>

In 2015, Sachdev et al. reported green synthesized CDs via hydrothermal treatment using coriander leaves in a yellow light brown aqueous system and successful showed ultraviolet (UV) light with bright green luminescence. The diameter of the CDs was approximately 4.158 nm and the quantum yield was 6.48%.<sup>[42]</sup> Similar results were reported by researchers that successfully used tea plants such as oolong tea<sup>[20]</sup> and waste tea<sup>[44]</sup> as a CD source.

In 2019, Shahshahanipour et al. used *Lawsonia inermis* as a carbon source to produce CDs without adding any chemical reagent for a size range of 3–7 nm and quantum yield with rhodamine B as the standard sample was 28.7%.<sup>[42]</sup> Some researchers reported green and ecofriendly synthesis from leaves using hydrothermal treatment for: *allium fistulosum*,<sup>[2]</sup> *Prosopis juliflora*,<sup>[46]</sup> purple perilla,<sup>[43]</sup> tulsi,<sup>[45]</sup> betel,<sup>[23]</sup> guava leaf extract,<sup>[24]</sup> *Hibiscus sabdariffa*,<sup>[50]</sup> *Boswellia ovalifoliolata* bark<sup>[49]</sup> and *Ocimum sanctum*.<sup>[48]</sup>

## 2.4 | Fruits

In 2018, Lu et al. reported versatile green synthesized nitrogen-doped carbon quantum dots (N-CQDs) by hydrothermal treatment using watermelon juice as a carbon precursor at 180°C for 3 h and showed excellent dispersibility and stability in water. N-CQDs had a size range of 3–7 nm with high fluorescence quantum yield of 10.6%.<sup>[76]</sup> Some CDs were synthesized from other fruits: orange juice,<sup>[68]</sup> strawberry juice,<sup>[74]</sup> *Lantana camara* berries,<sup>[65]</sup> ginkgo,<sup>[63]</sup> *Hylocereus undatus* (dragon fruit),<sup>[64]</sup> *Chionanthus retusus* extract,<sup>[60]</sup> *Actinidia deliciosa*,<sup>[59]</sup> and *Phyllanthus emblica*.<sup>[79]</sup> In 2016, Atchudan et al. reported CDs as nitrogen-doped (N-CDs) using unripe peach fruit and ammonia as the carbon precursor via a hydrothermal treatment for highly photoluminescent N-CDs. The mean size of the N-CDs was approximately 8 nm with quantum yield of 15%.<sup>[75]</sup> Atchudan et al. also reported N-CDs from fruits *Prunus mume*<sup>[80]</sup> and *Phyllanthus acidus*.<sup>[70]</sup>

In 2016, Jhonsi et al. reported tamarind as a carbon source for fluorescent carbon nanodots modified with triethylenetetramine (TCDs) and resulting size 1–3 nm, plus excitation-dependent emission with quantum yield 4%. The proposed mechanism for TCDs from tamarind was carbonization of the constituents that mainly consisted of sugar (12.5%), tartaric acid (5–8%), citric acid (0.64–3.95%), potassium tartrate (4.5–6%), and malic, formic, acetic, and butyric acids (trace amounts).<sup>[89]</sup>

Facile green synthesis of CDs from fruits was also reported for *Pyrus pyrifolia*,<sup>[72]</sup> *Prunus cerasifera*,<sup>[71]</sup> and banana juice.<sup>[90]</sup> In 2020, Senol et al. reported Seville orange (*Citrus aurantium*) as a carbon source for water-soluble CDs. The average particle sizes of the CDs were 4.8 nm and quantum yield 13.3%.<sup>[73]</sup>

In 2020, Chaudhary et al. reported green synthesis for highly fluorescent N,S co-doped CQDs (NS-CQDs) using banana (*Musa acuminata*) juice as a carbon precursor. Banana juice contains a high amount of carbohydrates: glucose, fructose, sucrose, and ascorbic acid. The average particle size of the NS-CQDs was 1.27 nm for blue fluorescence with a high quantum yield of 32%.<sup>[19]</sup> The reported sources for CQDs were fruits such as jujube,<sup>[22]</sup> lemon,<sup>[66]</sup> lemon peel,<sup>[84]</sup> *lycii fructus*,<sup>[67]</sup> orange waste peel<sup>[83]</sup> and red lentils.<sup>[77]</sup>

In 2015, Metha et al. reported apple juice as a carbon source via a one-step hydrothermal method for fabricating CDs at 150°C for 12 h and showed a good quantum yield of 4.27%. Apples also contain a wide variety of organic molecules (carbohydrates, polyphenols, and volatile organic compounds).<sup>[15]</sup> Other research on CDs with fruit and seeds as a source of carbon used jackfruit,<sup>[16]</sup> gardenia,<sup>[62]</sup> date kernel,<sup>[61]</sup> limeade,<sup>[91]</sup> papaya,<sup>[69]</sup> walnut oil,<sup>[81]</sup> pear juice,<sup>[21]</sup> areca nut husk,<sup>[85]</sup> black sesame seeds,<sup>[88]</sup> and *Sterculia lychnophora* seeds.<sup>[86]</sup>

In 2015, Kasibabu et al. prepared fluorescent CDs using carica papaya juice hydrothermally at different temperatures (125°C, 150°C, and 170°C) for 12 h. However, the best temperature was 170°C with a smaller size from 1.5 to 6.5 nm and good quantum yield of approximately 4.27%.<sup>[78]</sup>

In 2018, Ramar et al. used pomelo (*Citrus maxima* or *Citrus grandis*) juice as a carbon precursor for synthesizing undoped carbon

quantum dots (UCQDs) and N-doped carbon quantum dots (N-CQDs). The average particle sizes of the UCQDs were 3 nm and 70 nm for N-CQDs.<sup>[29]</sup>

### 3 | APPLICATION

#### 3.1 | Sensing

Fluorescence (FL)-based sensing has received much attention from scientists in recent years due to its excellent sensitivity, short response time, and low cost. Various fluorescent sensory materials have been designed and developed including organic dyes, quantum dots, metal-organic frameworks, and fluorescent proteins. However, each material offers not only advantages but also limitations and problems in implementation.<sup>[4]</sup>

CDs are widely used as chemical sensors for bioactive molecules due to their small size, low cytotoxicity, and easy incorporation of surface functional groups. Sensing mechanisms shown in Figure 2 demonstrate CDs for fluorescence quenching. The basic principles of fluorescence quenching are as follows: (a) CDs can donate photoexcited electrons to the conduction band of metal ions (electron transfer, positron emission tomography (PET) mechanisms); (b) transfer of energy from the excited state of CDs to metal ions (fluorescence resonance energy transfer, FRET); (c) reabsorbed energy emitted from CDs by metal ions (inner filter effect, IFE); (d) CDs donate photoexcited electrons to the vacant d orbital of metal ions; (e) during aggregation of CDs, energy from the excited CDs is transferred to the ground state without radiative emission (aggregation induced emission quenching, AIEQ); and (f) CDs form complexes with metal ion

quenchers in the ground state and undergo nonradiative emission (static quenching effect, SQE). These pathways are dynamic quenching mechanisms except for SQE.<sup>[92]</sup>

Recently, CD-induced CL systems have generated great interest due to their nontoxic, biocompatible, and environmentally friendly nature. It has been reported that heteroatom doping will improve the optical properties of CDs, especially quantum yield (QY) and is widely applicable in chemical and biological sensing.<sup>[93]</sup> In 2011, Lin et al. reported fluorescent CDs and successfully demonstrated chemiluminescence (CL) in the presence of ONOOH formed by mixing acidified  $H_2O_2$  and  $NaNO_2$ . They found a linear relationship between nitrite formation of ONOOH and the CL signal produced from the carbon dots- $NaNO_2$ - $H_2O_2$  system. The CL system has been developed as a sensitive and convenient method for determination of nitrite in pond water, river water, and pure milk.<sup>[94]</sup>

Ferric ions ( $Fe^{3+}$ ) are metal ions with many roles in biological systems and living organisms and can be found easily in nature. However, excessive amounts of  $Fe^{3+}$  ions in the human body can cause various diseases. In 2017, Shah et al. reported that N-CDs produced via the Fenton reaction improved  $H_2O_2$  efficiency and promoted the generation of  $\bullet OH$  radicals that resulted in enhanced CL emission from the Fenton system. The high CL intensity of this system for the response to  $Fe^{2+}$  may due to peroxide-induced autoxidation of  $Fe^{2+}$  in acidic medium.<sup>[95]</sup> A sensing method for the detection of  $Fe^{2+}$  ions in solution was developed via CL using N-CDs/ $H_2O_2$ .  $Fe^{2+}$  ions have the ability to generate  $\bullet OH$  from hydrogen peroxide ( $H_2O_2$ ). Therefore, a mixed N-CDs/ $H_2O_2$  solution was utilized for selective quantification of  $Fe^{2+}$  ions in solution and showed that CL emission intensity increased with increasing concentrations of  $Fe^{2+}$ .<sup>[96]</sup>

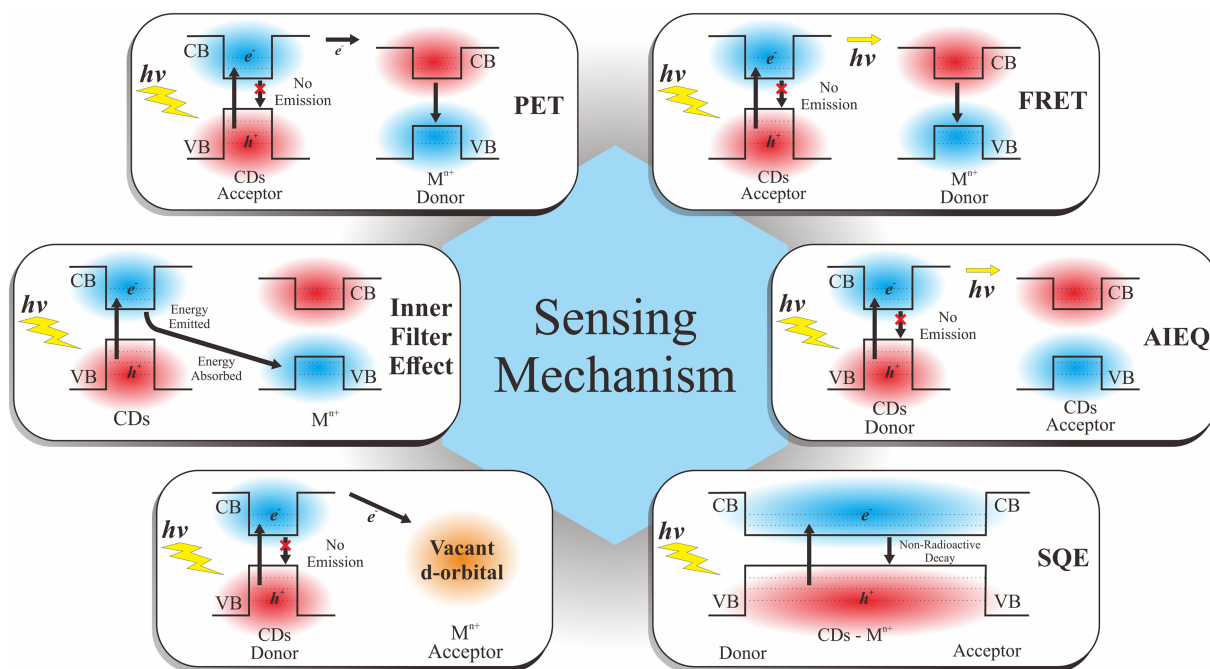


**FIGURE 2** Sensing mechanisms of CDs by fluorescence quenching based on the following basic principles<sup>[92]</sup>

In 2019, Geetha et al. reported synthesized CDs using *Boswellia ovalifoliolata* bark extract as the carbon source from leaves to detect  $\text{Fe}^{3+}$  and led to fluorescent quenching via the electron transfer mechanism. The synthesized CDs revealed a good QY of 10.2% and could be used as a fluorescent probe for detection of  $\text{Fe}^{3+}$  in aqueous solution with high sensitivity and selectivity and a detection limit of  $0.41 \mu\text{M}$ .<sup>[49]</sup> Similar results were reported by other studies using leaves of betel<sup>[23]</sup> and coriander<sup>[42]</sup> as carbon sources.

Another plant part that is also used as a detector for  $\text{Fe}^{3+}$  ions is the bulb. Novel fluorescent nitrogen and sulfur co-doped carbon dots (N, S, CDs) were synthesized from garlic for detection of  $\text{Fe}^{3+}$  ions using hydroxyl groups on the surface of the CDs, as described by Chen et al. in 2016. This led to fluorescent quenching via the PET or FRET mechanism with a detection limit of  $0.22 \text{ nM}$ .<sup>[3]</sup> Some researchers also reported sensing through other types of bulbs from rose-heart radish<sup>[32]</sup> and sweet potato.<sup>[1]</sup>

Fruit is a part of the plant that is also used as a carbon source of CDs for sensing  $\text{Fe}^{3+}$ . CQDs were synthesized from jujubes using PET by Kim et al. in 2018 with a sensing ability in the range  $0\text{--}200 \text{ M}$ . Other studies on carbon sources for sensing applied fruit such as *Chionanthus retusus*,<sup>[60]</sup> grape peel,<sup>[82]</sup> *lycii fructus*,<sup>[67]</sup> papaya,<sup>[69]</sup> *Prunus cerasifera*,<sup>[71]</sup> red lentils,<sup>[77]</sup> Seville orange,<sup>[73]</sup> watermelon juice,<sup>[76]</sup> and *Phyllanthus acidus*.<sup>[70]</sup>

Flowers are also used as a source of CDs for detection of  $\text{Fe}^{3+}$  ions. In 2018, Atchudan et al. successfully synthesized N-CDs using *Magnolia liliiflora* flowers for detection of  $\text{Fe}^{3+}$  ions by forming the complex N-CDs- $\text{Fe}^{3+}$  and by maximizing functional groups such as nitrogen, carbonyl, and carboxyl on the surface of N-CDs and with a detection limit of  $1.2 \mu\text{M}$ .<sup>[36]</sup>

Copper ions ( $\text{Cu}^{2+}$ ) are the most abundant essential transition metal ions in the human body in addition to zinc and iron ions and play a very important role in living organisms. However, excess doses are highly toxic to organisms and  $\text{Cu}^{2+}$  is listed as a priority pollutant by the United States Environmental Protection Agency (US EPA).<sup>[47]</sup> To control  $\text{Cu}^{2+}$  pollution and its toxic effects, there has been a great demand for simple, green, reliable and sensitive strategies for coating the CQDs with branched polyethyleneimine (BPEI) by electrostatic adsorption to produce BPEI-capped CQDs (BPEI-CQDs). BPEI-CQDs resulted in a limit of detection (LOD) of  $115 \text{ nm}$  and a dynamic range from  $0.333$  to  $66.6 \mu\text{M}$ . In addition, BPEI-CQDs were successfully used to detect  $\text{Cu}^{2+}$  in river water. CQDs have been synthesized from bamboo leaves as a carbon source with the inner filter effect as a sensing mechanism.<sup>[48]</sup> In 2017, Shi et al. synthesized nitrogen-doped carbon nanodots (N-CDs) using oolong tea as the carbon source for  $\text{Cu}^{2+}$  detection via the SQE in aqueous solution with a linear range of  $0.01\text{--}75 \mu\text{M}$  and a detection limit of  $2 \mu\text{M}$ . SQE methods were also reported using pear juice<sup>[20]</sup> and for FRET using banana juice.<sup>[19]</sup>

One heavy metal ion (mercury ion [ $\text{Hg}^{2+}$ ]) is toxic for aquatic ecosystems. Pollution with mercury ions is through drinking water and food, and in the human body can lead to brain damage and other chronic diseases. Some scientists are developing research to detect mercury ions using CDs. In 2017, Li et al. reported nitrogen-doped carbon dots (N-CDs) from orange juice as the carbon precursor for

detection of mercury ions ( $\text{Hg}^{2+}$ ) using the SQE sensing mechanism. The interaction ratio of N-CDs was proportional to the concentration of  $\text{Hg}^{2+}$  at approximately  $4.0 \mu\text{g/ml}$  and recovery was in the range  $102\text{--}103\%$  that indicated good sensitivity and accuracy for  $\text{Hg}^{2+}$  detection.<sup>[68]</sup>

In 2019, Pourezza et al. used *Prosopis juliflora* leaves as a carbon source for synthesizing CQDs for sensing and selective  $\text{Hg}^{2+}$  detection with a detection limit of  $1.26 \text{ ng ml}^{-1}$ .<sup>[46]</sup> Some studies for  $\text{Hg}^{2+}$  detection using CDs from plants investigated Hong Cailai<sup>[51]</sup> and gardenia fruit.<sup>[62]</sup>

Chromium (Cr) has received special attention among heavy metals because of its toxicity and carcinogenic properties. The hexavalent chromium ion ( $\text{Cr}^{6+}$ ) is a common species in the environment but at permissible levels becomes a micronutrient and is nontoxic for humans. However, hexavalent chromium ion ( $\text{Cr}^{6+}$ ) concentrations that exceed the allowable limit have harmful long-term side effects on humans and animals. As with ferrous, copper, and mercury metal ions, CDs from plants can also be used to detect  $\text{Cr}^{6+}$  ions. In 2018, Bhatt et al. reported CDs from tulsi leaves for selective and sensing  $\text{Cr}^{6+}$  with a detection limit of  $4.5 \text{ ppb}$  and linear static quenching was observed from  $1.6 \mu\text{M}$  to  $50 \mu\text{M}$ .<sup>[45]</sup>

In 2019, Roshni et al. synthesized nitrogen-doped carbon dots (N-CDs) from peanuts for sensing  $\text{Cr}^{6+}$  ions with a detection limit of  $0.1 \text{ mg/L}$ .<sup>[30]</sup> Other CDs from plants have been used for  $\text{Cr}^{6+}$  detection, for example from enokitake mushroom<sup>[54]</sup> and hibiscus sabdariffa leaves.<sup>[50]</sup> Some studies also reported sensing applications via plants such as lemon fruit,<sup>[66]</sup> broccoli,<sup>[40]</sup> lantana camara berries,<sup>[65]</sup> purple perilla,<sup>[43]</sup> *Pyrus pyrifolia*,<sup>[72]</sup> *Nigella sativa* seeds,<sup>[39]</sup> and *Ocimum sanctum*.<sup>[48]</sup>

### 3.2 | Imaging

CDs for imaging applications may be through high-water solubility, photostability, and photobleaching resistivity.<sup>[92]</sup> In 2018, Amin et al. reported fluorescent N-CDs synthesized from the date kernel for *in vitro* bio imaging.<sup>[61]</sup> Cellular toxicity of the N-CDs was investigated using human MG-63 cells and demonstrated low cytotoxicity and excellent membrane permeability with strong green fluorescence. Cytotoxicity plays a key role in determining the applicability of nanoparticles as fluorescence imaging agents.<sup>[42]</sup> In 2015, Sachdev et al. used coriander leaves to synthesize CDs for normal lung (L-132) and cancer (A549) cell lines, which exhibited green fluorescence.<sup>[42]</sup>

In 2015, Feng et al. successfully synthesized N-CDs from winter melon for *in vitro* bioimaging and showed blue fluorescence in hepG2 cells at  $405 \text{ nm}$  excitation using confocal laser microscopic imaging.<sup>[87]</sup> In 2016, Atchudan et al. reported N-CDs extracted from *Prunus persica* (peach) as the carbon precursor that exhibited a high QY, low cytotoxicity, and showed blue fluorescence.<sup>[75]</sup> Fruits reported that exhibited blue fluorescence were *Abelmoschus manihot*<sup>[35]</sup> and watermelon.<sup>[76]</sup>

In 2017, Sun et al. reported *lycii fructus* as a carbon source for synthesis of CDs that were applied to HeLa cells and exhibited low

cytotoxicity, good biocompatibility, and showed blue and green fluorescence.<sup>[67]</sup> In 2019, Ma et al. prepared a facile synthesis of fluorescent CDs from *Prunus cerasifera* fruits and these were found to have low toxicity for HepG2 cells, which exhibited blue and green fluorescence under a fluorescence microscope.<sup>[71]</sup> Other natural sources for CDs with blue and green fluorescence are ginkgo fruits,<sup>[63]</sup> orange juice,<sup>[18]</sup> *Prunus mume*,<sup>[80]</sup> and *Actinidia deliciosa*.<sup>[59]</sup>

Liu et al. in 2017 reported blue, green, and red fluorescence via a low-cost synthesis route for fabrication of N-CDs using rose-heart radish and had good biocompatibility. In 2017, Shen et al. successfully synthesized CDs from sweet potato for cell imaging using HeLa cells and HepG2 cells and indicated that the CDs showed good fluorescence with a QY of approximately 8.64%. Other CDs reported to exhibit green, blue and red fluorescence from natural sources were synthesized from *Magnolia liliiflora*,<sup>[36]</sup> *Phyllanthus acidus*,<sup>[70]</sup> cabbage,<sup>[17]</sup> *Hibiscus sabdariffa*,<sup>[50]</sup> hong caitai,<sup>[52]</sup> and tulsi leaves.<sup>[45]</sup>

For biomedical applications using nanomaterials such as metal nanoclusters (NCs) and ultrasmall noble metal nanoparticles (UNMNPs), the materials produced typically had diameters less than 2 nm and offer the missing link between metal atoms and nanoparticles, or even bulk noble metals. The unique properties of biofunctionalized scaffolds to protect metal nanoclusters in combination with their ultrasmall size and good biocompatibility for emerging functional materials has been applied in various biomedical fields.<sup>[97]</sup> Metal nanoclusters (MNCs) as bioimaging agents have characteristics of deep tissue penetration, and reduced photodamage and background interference.<sup>[98]</sup>

The physicochemical properties of metal NCs for biomedical applications lend their use as theranostic agents in cancer therapy, imaging-guided therapy, antimicrobial agents, and bioimaging.<sup>[99]</sup> Zheng et al. in 2020 developed a full spectrum of alloy metal nanoclusters (NCs),  $Au_xAg_{25-x}(MHA)_{18}$  (where MHA = 6-mercaptohexanoic acid) with  $x = 0-25$ , and investigated their composition-dependent antimicrobial performance and showed the stability that might play a key role for intracellular or *in vivo* fate biomedical applications.<sup>[100]</sup>

Jiang et al. in 2019 reported the strong NIR absorption of  $Au_{25}(SG)_{18}$  nanoclusters and successfully used these for photoacoustic (PA) imaging to *in situ* visualize their transport through the aorta to the renal parenchyma and subsequent filtration into the renal pelvis at a temporal resolution down to 1 s.<sup>[101]</sup> Ultrasmall gold nanoclusters (Au NCs) with a particle size of  $\sim 1$  nm are emerging as promising nanoparticles due to their structure, unique physicochemical properties, facile surface functionalization, and good biocompatibility<sup>[102]</sup>; they have many unique advantages and exhibit great potential in biomedical research.<sup>[103]</sup>

### 3.3 | Drug delivery

The advantages of CDs are biocompatibility, reduced toxic, biodegradability, and easy synthesis, and indicated that they are the best candidates for drug delivery.<sup>[38]</sup> Shao et al. in 2020 successfully synthesized CDs from mulberry leaf (*Morus alba* L.) residues for use

with the drug Lycorine and these have also been successfully applied for simultaneous intracellular imaging and anticancer cell activity.<sup>[58]</sup> John et al. in 2019 also prepared CDs using wheat bran as a drug delivery agent for amoxicillin (AMX); at different pH (5.0, 6.8 and 7.2) it was an antibacterial drug delivery agent with minimal cytotoxic effects.<sup>[38]</sup>

D'Souza et al. in 2017 reported a one-step ecofriendly method for the fabrication of fluorescent CDs using *Daucus carota* subsp. *sativus* (carrot) roots as a carbon source for mitomycin drug loading. They also found that ultrasmall sized CDs could exhibit high affinity towards the cancer cell membrane for internalization of mitomycin-CDs by *Bacillus subtilis* cells.<sup>[28]</sup> Figure 3 shows the mechanism of CDs as a drug delivery system together with sensing applications. Ganguly et al. in 2019 reported microwave-assisted green synthesis of zwitterionic photoluminescent N-doped CDs for efficient chemosensors with tracer  $Cr^{6+}$  by considering the inner filter effect and nano drug delivery.<sup>[104]</sup>

### 3.4 | Catalysis

For photocatalyst applications, CDs are highly recommended due to their air solubility, chemical stability, and low toxicity compared with other common photocatalysts materials: ZnO,  $TiO_2$ , and CdS. The CDs also have properties of excellent absorbance and optical photoluminescence (PL) and also the most important property for photocatalysts, which is tunable modification at the surface. An

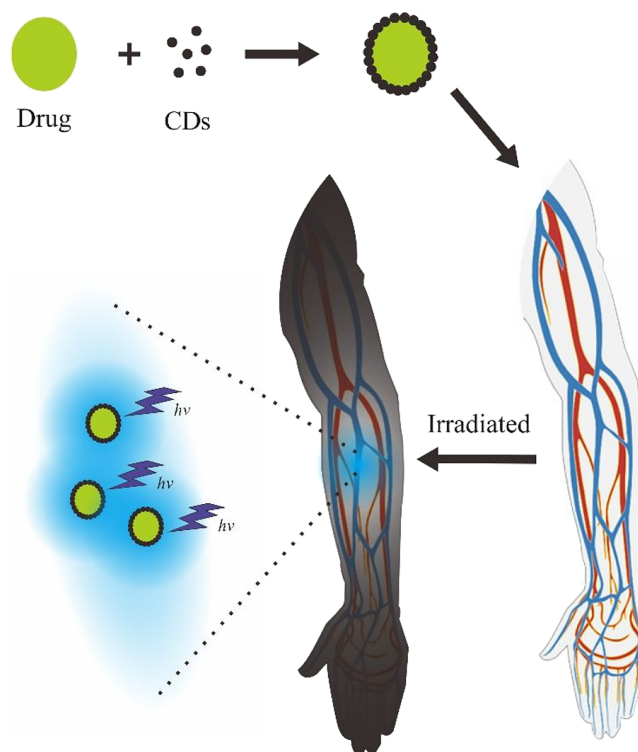


**FIGURE 3** Illustration of CDs mechanism for drug delivery along with sensing applications<sup>[104]</sup>

optical phenomenon of CDs is upconversion PL (UCPL), which is suitable for absorbing visible region due to the ability to emit light at shorter wavelengths than the semiconductor bandwidth. CDs provide efficient electron and hole separation because photoinduced CDs are excellent electron donors and acceptors.<sup>[105]</sup> The mechanisms of photocatalysis by CDs shown in Figure 4 are based on the following principles: (a)  $\pi$ -conjugated CDs can act as sensitizers by donating their photoexcited electrons to the conduction band of metal/metal oxides under visible light irradiation<sup>[106–108]</sup>; (b) CDs can act as an electron reservoir to inhibit  $e^-/h^+$  recombination by accepting photoexcited electrons from metal/metal oxides<sup>[106,108,109]</sup> (c) CDs can bond with organic dyes by  $\pi$ - $\pi^*$  interaction that increases the degradation performance; and (d) CDs with upconversion photoluminescence can absorb light in the visible wavelength and emit ultraviolet light to form photoexcited electrons.<sup>[92]</sup>

Prasannan et al. in 2013 reported photocatalytic ZnO-loaded CDs synthesized from orange waste peels for naphthol black-blue azo (NBBA) dye under UV irradiation.<sup>[74]</sup> The CDs could act as reservoirs to trap electrons emitted from ZnO to avoid electron hole recombination. Electrons in the reservoir could react with oxygen to produce superoxide radicals ( $O_2^-$ ) and holes react with water to produce hydroxyl radicals (OH). The radicals would break the bond in the NBBA dye molecule to produce harmless products.<sup>[83]</sup> Lemon peel was also used by Tyagi et al. in 2016 as a source of carbon for water-soluble CQDs (wsCQDs). The composite wsCQDs and  $TiO_2$  nanofibres was developed at room temperature using 6-aminohexanoic acid as a linking molecule for photocatalytic degradation of methylene blue (MB) dye and was found to be approximately 2.5 times higher than that of  $TiO_2$  nanofibres.<sup>[84]</sup>

Arul et al. in 2018 prepared N-CDs using *Actinidia deliciosa* to act as a catalyst using additional sodium borohydride ( $NaBH_4$ ) in the degradation of dyestuff rhodamine B (RhB). UV-visible spectroscopy was

used to analyze degradation performance at 554 nm and showed degradation of RhB due to electron transfer and energy barrier reduction between the reactants and products that was mediated by N-CDs.<sup>[59]</sup> Arul et al. in 2017 also reported sodium borohydride ( $NaBH_4$ ) for degradation of the dye MB by additional N-CDs that were synthesized from *H. undatus* fruits and N-CDs. They successfully showed excellent catalytic activity in that  $BH_4^-$  from  $NaBH_4$  and MB were absorbed on the N-CD surface.<sup>[64]</sup>

Quantum CDs (UCQDs) and N-doped quantum CDs (N-CQDs) from *Citrus grandis* were reported by Ramar et al. for photocatalysts for MB dye under direct sunlight radiation. At the surface of the catalyst (CQDs), MB dye adsorbed energy from sunlight and electrons in the valence band were excited to the conduction band of the CQDs and remaining holes in the valence band.<sup>[106–109]</sup> Sunlight has an important role in photo-oxidation and photosensitizing reaction mechanisms in CQDs as efficient photocatalysts.<sup>[29]</sup>

## 4 | CONCLUSION

Carbon dots (CDs) have been shown at sizes less than 10 nm to have excellent photostability, biocompatibility, low toxicity, and good solubility. The synthesized CDs contain hydroxyl, carboxyl or epoxy groups that are produced from the oxidation of oligosaccharide and aliphatic chains from various carbon sources or precursors that are attached on the surface of the CDs. Natural materials have been widely used as carbon sources for the synthesis of CDs derived from plant parts such as bulbs, flowers, leaves, and fruit. The hydrothermal method was reported most by researchers due to its convenience, and also being environmentally friendly and low cost. CDs that have good properties have been widely applied in various fields including sensing, imaging, drug delivery, and as catalysts.

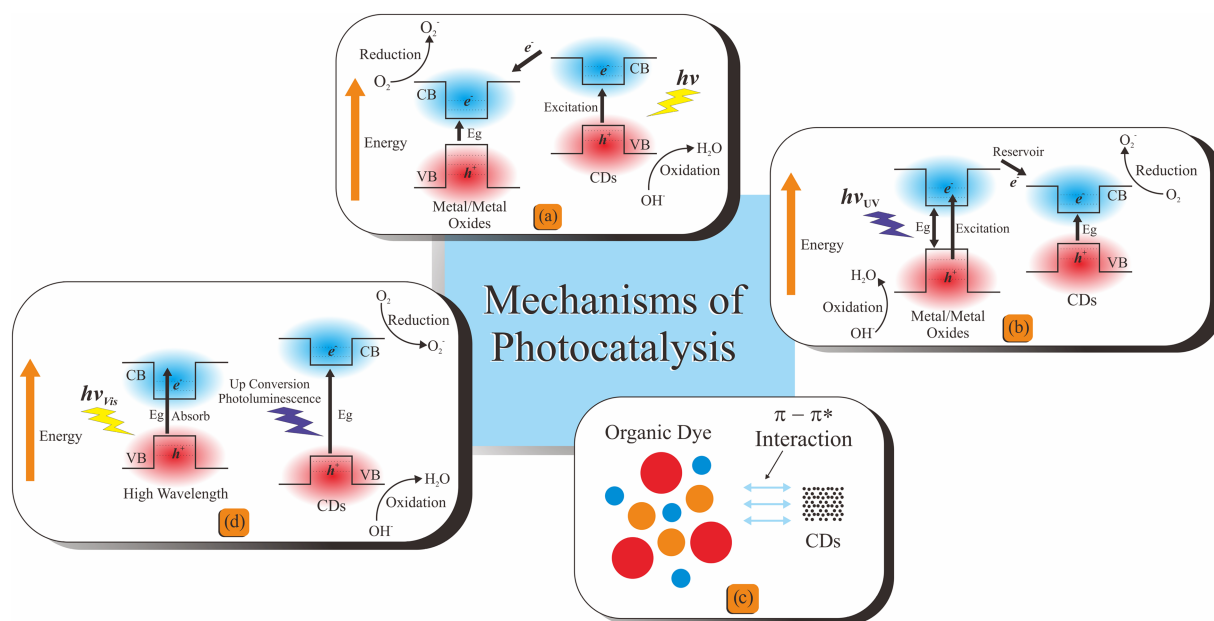


FIGURE 4 Illustration of mechanisms of photocatalysis by CDs<sup>[92]</sup>

## ACKNOWLEDGEMENTS

This work was supported by the Penelitian Dasar (PD) and Penelitian Terapan (PT) funded by the Indonesian Government (Kemenristek/BRIN) grants: 1516/UN4.22/PT.01.03/2021.

## ORCID

Dahlang Tahir  <https://orcid.org/0000-0002-8241-3604>

## REFERENCES

- [1] J. Shen, S. Shang, X. Chen, D. Wang, Y. Cai, *Mater. Sci. Eng. C* **2017**, *76*, 856.
- [2] Z. Wei, B. Wang, Y. Liu, Z. Liu, H. Zhang, S. Zhang, J. Chang, S. Lu, *New J. Chem.* **2019**, *43*, 718.
- [3] Y. Chen, Y. Wu, B. Weng, B. Wang, C. Li, *Sens. Actuators B* **2016**, *223*, 689.
- [4] X. Sun, Y. Lei, *TrAC - Trends Anal. Chem.* **2017**, *89*, 163.
- [5] H. M. Ahmed, M. Ghali, W. K. Zahra, M. Ayad, *Mater. Today Proc.* **2020**, *33*, 1845.
- [6] S. N. A. Shah, J. M. Lin, *Adv. Colloid Interface Sci.* **2017**, *241*, 24.
- [7] W. Xue, Z. Lin, H. Chen, C. Lu, J. M. Lin, *J. Phys. Chem. C* **2011**, *115*, 21707.
- [8] S. N. A. Shah, H. Li, J. M. Lin, *Talanta* **2016**, *153*, 23.
- [9] Y. Zheng, D. Zhang, S. N. A. Shah, H. Li, J. M. Lin, *Chem. Commun.* **2017**, *53*, 5657.
- [10] P. Miao, K. Han, Y. Tang, B. Wang, T. Lin, W. Cheng, *Nanoscale* **2015**, *7*, 1586.
- [11] X. Song, W. Zhu, X. Ge, R. Li, S. Li, X. Chen, J. Song, J. Xie, X. Chen, H. Yang, *Angew. Chemie Int. Ed.* **2021**, *60*, 1306.
- [12] K. Zheng, M. I. Setyawati, D. T. Leong, J. Xie, *Nano Res.* **2021**, *14*, 1026.
- [13] H. Liu, G. Hong, Z. Luo, J. Chen, M. Gong, H. He, J. Yang, X. Yuan, L. Lin, X. Mu, J. Wong, W. Mi, J. Luo, J. Xie, X. Zhang, *Adv. Mater.* **2019**, *31*, 1.
- [14] Q. Huang, Q. Li, Y. Chen, L. Tong, X. Lin, J. Zhu, Q. Tong, *Sens. Actuators B* **2018**, *276*, 82.
- [15] V. N. Mehta, S. Jha, H. Basu, R. K. Singhal, S. K. Kailasa, *Sens. Actuators B* **2015**, *213*, 434.
- [16] N. Thongsai, P. Jaiyong, S. Kladsomboon, I. In, P. Paoprasert, *Appl. Surf. Sci.* **2019**, *487*, 1233.
- [17] A. M. Alam, B. Y. Park, Z. K. Ghouri, M. Park, H. Y. Kim, *Green Chem.* **2015**, *17*, 3791.
- [18] S. Sahu, B. Behera, T. K. Maiti, S. Mohapatra, *Chem. Commun.* **2012**, *48*, 8835.
- [19] N. Chaudhary, P. K. Gupta, S. Eremin, P. R. Solanki, *J. Environ. Chem. Eng.* **2020**, *8*, 103720.
- [20] L. Shi, B. Zhao, X. Li, G. Zhang, Y. Zhang, C. Dong, S. Shuang, *Anal. Methods* **2017**, *9*, 2197.
- [21] L. Liu, H. Gong, D. Li, L. Zhao, *J. Nanosci. Nanotechnol.* **2018**, *18*, 5327.
- [22] K. Kim, J. Kim, *J. Nanosci. Nanotechnol.* **2018**, *18*, 1320.
- [23] D. Raja, D. Sundaramurthy, *Mater. Today Proc.* **2021**, *34*, 488.
- [24] R. Ramanarayanan, S. Swaminathan, *Mater. Today Proc.* **2020**, *33*, 2223.
- [25] X. Yang, D. Wang, N. Luo, M. Feng, X. Peng, X. Liao, *Spectrochim. Acta Part A Mol. Biomol. Spectrosc.* **2020**, *239*, 118462.
- [26] S. Irvani, *Green Chem.* **2011**, *13*, 2638.
- [27] R. R. Nasaruddin, T. Chen, Q. Yao, S. Zang, J. Xie, *Coord. Chem. Rev.* **2021**, *426*, 213540.
- [28] S. L. D'Souza, S. S. Chettiar, J. R. Koduru, S. K. Kailasa, *Optik (Stuttg.)* **2018**, *158*, 893.
- [29] V. Ramar, S. Moothattu, K. Balasubramanian, *Sol. Energy* **2018**, *169*, 120.
- [30] V. Roshni, S. Misra, M. K. Santra, D. Ootoor, *J. Photochem. Photobiol. A* **2019**, *373*, 28.
- [31] J. X. Zheng, X. H. Liu, Y. Z. Yang, X. G. Liu, B. S. Xu, *Xinxing Tan Cailiao/New Carbon Mater.* **2018**, *33*, 276.
- [32] W. Liu, H. Diao, H. Chang, H. Wang, T. Li, W. Wei, *Sens. Actuators B* **2017**, *241*, 190.
- [33] S. Zhao, M. Lan, X. Zhu, H. Xue, T. W. Ng, X. Meng, C. S. Lee, P. Wang, W. Zhang, *ACS Appl. Mater. Interfaces* **2015**, *7*, 17054.
- [34] Y. Hu, L. Zhang, X. Li, R. Liu, L. Lin, S. Zhao, *ACS Sustain. Chem. Eng.* **2017**, *5*, 4992.
- [35] Y. Wan, M. Wang, K. Zhang, Q. Fu, M. Gao, L. Wang, Z. Xia, D. Gao, *Microchem. J.* **2019**, *148*, 385.
- [36] R. Atchudan, T. N. J. I. Edison, K. R. Aseer, S. Perumal, Y. R. Lee, *Colloids Surf. B Biointerfaces* **2018**, *169*, 321.
- [37] H. Diao, T. Li, R. Zhan, Y. Kang, W. Liu, Y. Cui, S. Wei, N. Wang, L. Li, H. Wang, W. Niu, T. Sun, *Spectrochim. Acta - Part A Mol. Biomol. Spectrosc.* **2018**, *200*, 226.
- [38] T. S. John, P. K. Yadav, D. Kumar, S. K. Singh, S. H. Hasan, *Luminescence* **2020**, *35*, 913.
- [39] N. Sharma, K. Yun, *Dyes. Pigm.* **2020**, *182*, 108640.
- [40] N. Arumugam, J. Kim, *Mater. Lett.* **2018**, *219*, 37.
- [41] Y. Song, X. Yan, Z. Li, L. Qu, C. Zhu, R. Ye, S. Li, D. Du, Y. Lin, *J. Mater. Chem. B* **2018**, *6*, 3181.
- [42] A. Sachdev, P. Gopinath, *Analyst* **2015**, *140*, 4260.
- [43] X. Zhao, S. Liao, L. Wang, Q. Liu, X. Chen, *Talanta* **2019**, *201*, 1.
- [44] K. Chen, W. Qing, W. Hu, M. Lu, Y. Wang, X. Liu, *Spectrochim. Acta Part A Mol. Biomol. Spectrosc.* **2019**, *213*, 228.
- [45] S. Bhatt, M. Bhatt, A. Kumar, G. Vyas, T. Gajaria, P. Paul, *Colloids Surf. B Biointerf.* **2018**, *167*, 126.
- [46] N. Pourreza, M. Ghomi, *Mater. Sci. Eng. C* **2019**, *98*, 887.
- [47] Y. Liu, Y. Zhao, Y. Zhang, *Sens. Actuators B* **2014**, *196*, 647.
- [48] A. Kumar, A. R. Chowdhuri, D. Laha, T. K. Mahto, P. Karmakar, S. K. Sahu, *Sens. Actuators B* **2017**, *242*, 679.
- [49] G. Venkatesan, V. Rajagopalan, S. N. Chakravarthula, *J. Environ. Chem. Eng.* **2019**, *7*, 103013.
- [50] L. Komalavalli, P. Amutha, S. Monisha, *Mater. Today Proc.* **2020**, *33*, 2279.
- [51] M. Shahshahanipour, B. Rezaei, A. A. Ensa, Z. Etemadifar, *Mater. Sci. Eng. C* **2019**, *98*, 826.
- [52] L. S. Li, X. Y. Jiao, Y. Zhang, C. Cheng, K. Huang, L. Xu, *Sens. Actuators B* **2018**, *263*, 426.
- [53] X. Xu, L. Cai, G. Hu, L. Mo, Y. Zheng, C. Hu, B. Lei, X. Zhang, Y. Liu, J. Zhuang, *JOL* **2020**, *227*, 117534.
- [54] M. R. Pacquiao, M. D. G. de Luna, N. Thongsai, S. Kladsomboon, P. Paoprasert, *Appl. Surf. Sci.* **2018**, *453*, 192.
- [55] H. Xu, X. Yang, G. Li, C. Zhao, X. Liao, *J. Agric. Food Chem.* **2015**, *63*, 6707.
- [56] S. Godavarthi, K. M. Kumar, E. V. Vélez, A. Hernandez-Eligio, M. Mahendhiran, N. Hernandez-Como, M. Aleton, L. M. Gomez, *J. Photochem. Photobiol. B Biol.* **2017**, *172*, 36.
- [57] A. Bayat, S. Masoum, E. S. Hosseini, *J. Mol. Liq.* **2019**, *281*, 134.
- [58] Y. Shao, C. Zhu, Z. Fu, K. Lin, Y. Wang, Y. Chang, L. Han, H. Yu, F. Tian, *J. Nanopart. Res.* **2020**, *22*, 1.
- [59] V. Arul, M. G. Sethuraman, *Opt. Mater. (Amst.)* **2018**, *78*, 181.
- [60] R. Atchudan, T. N. J. I. Edison, D. Chakradhar, S. Perumal, J. J. Shim, Y. R. Lee, *Sens. Actuators B* **2017**, *246*, 497.
- [61] N. Amin, A. Afkhami, L. Hosseinzadeh, T. Madrakian, *Anal. Chim. Acta* **2018**, *1030*, 183.
- [62] D. Sun, T. Liu, C. Wang, L. Yang, S. Yang, K. Zhuo, *Spectrochim. Acta Part A Mol. Biomol. Spectrosc.* **2020**, *240*, 118598.
- [63] L. Li, L. Li, C. P. Chen, F. Cui, *Inorg. Chem. Commun.* **2017**, *86*, 227.
- [64] V. Arul, T. N. J. I. Edison, Y. R. Lee, M. G. Sethuraman, *J. Photochem. Photobiol. B Biol.* **2017**, *168*, 142.

- [65] R. Bandi, R. Dadigala, B. R. Gangapuram, V. Guttena, *J. Photochem. Photobiol. B Biol.* **2018**, *178*, 330.
- [66] B. T. Hoan, T. T. Thanh, P. D. Tam, N. N. Trung, S. Cho, V. H. Pham, *Mater. Sci. Eng. B Solid-State Mater. Adv. Technol.* **2019**, *251*, 114455.
- [67] X. Sun, J. He, S. Yang, M. Zheng, Y. Wang, S. Ma, H. Zheng, *J. Photochem. Photobiol. B Biol.* **2017**, *175*, 219.
- [68] Z. Li, Y. Zhang, Q. Niu, M. Mou, Y. Wu, X. Liu, Z. Yang, S. Liao, *JOL* **2017**, *187*, 274.
- [69] N. Wang, Y. Wang, T. Guo, T. Yang, M. Chen, J. Wang, *Biosens. Bioelectron.* **2016**, *85*, 68.
- [70] R. Atchudan, T. N. J. I. Edison, K. R. Aseer, S. Perumal, N. Karthik, Y. R. Lee, *Biosens. Bioelectron.* **2018**, *99*, 303.
- [71] H. Ma, C. Sun, G. Xue, G. Wu, X. Zhang, X. Han, X. Qi, X. Lv, H. Sun, J. Zhang, *Spectrochim. Acta - Part A Mol. Biomol. Spectrosc.* **2019**, *213*, 281.
- [72] J. R. Bhamore, S. Jha, R. K. Singhal, T. J. Park, S. K. Kailasa, *J. Mol. Liq.* **2018**, *264*, 9.
- [73] A. M. Senol, E. Bozkurt, *Microchem. J.* **2020**, *159*, 105357.
- [74] H. Huang, J. J. Lv, D. L. Zhou, N. Bao, Y. Xu, A. J. Wang, J. J. Feng, *RSC Adv.* **2013**, *3*, 21691.
- [75] R. Atchudan, T. N. J. I. Edison, Y. R. Lee, *J. Colloid Interface Sci.* **2016**, *482*, 8.
- [76] M. Lu, Y. Duan, Y. Song, J. Tan, L. Zhou, *J. Mol. Liq.* **2018**, *269*, 766.
- [77] Z. M. S. H. Khan, R. S. Rahman, S. Islam, M. Zulfequar, *Opt. Mater. (Amst.)* **2019**, *91*, 386.
- [78] B. S. B. Kasibabu, S. L. D'Souza, S. Jha, S. K. Kailasa, *J. Fluoresc.* **2015**, *25*, 803.
- [79] V. Arul, M. G. Sethuraman, *ACS Omega* **2019**, *4*, 3449.
- [80] R. Atchudan, T. N. J. I. Edison, M. G. Sethuraman, Y. R. Lee, *Appl. Surf. Sci.* **2016**, *384*, 432.
- [81] E. Arkan, A. Barati, M. Rahmanpanah, L. Hosseinzadeh, S. Moradi, M. Hajialyani, *Adv. Pharm. Bull.* **2018**, *8*, 149.
- [82] J. Xu, T. Lai, Z. Feng, X. Weng, C. Huang, *Luminescence* **2015**, *30*, 420.
- [83] A. Prasannan, T. Imae, *Ind. Eng. Chem. Res.* **2013**, *52*, 15673.
- [84] A. Tyagi, K. M. Tripathi, N. Singh, S. Choudhary, R. K. Gupta, *RSC Adv.* **2016**, *6*, 72423.
- [85] J. Mathew, J. Joy, S. A. Kumar, J. Philip, *JOL* **2019**, *208*, 356.
- [86] F. Qu, H. Pei, R. Kong, S. Zhu, L. Xia, *Talanta* **2017**, *165*, 136.
- [87] X. Feng, Y. Jiang, J. Zhao, M. Miao, S. Cao, J. Fang, L. Shi, *RSC Adv.* **2015**, *5*, 31250.
- [88] P. Supchocksoonthorn, N. Thongsai, H. Moonmuang, S. Kladsomboon, P. Jaiyong, P. Paoprasert, *Colloids Surf. A Physicochem. Eng. Asp.* **2019**, *575*, 118.
- [89] M. Asha Jhonsi, S. Thulasi, *Chem. Phys. Lett.* **2016**, *661*, 179.
- [90] B. De, N. Karak, *RSC Adv.* **2013**, *3*, 8286.
- [91] P. Suvarnaphaet, C. S. Tiwary, J. Wetcharungsri, S. Porntheeraphat, R. Hoonsawat, P. M. Ajayan, I. M. Tang, P. Asanithi, *Mater. Sci. Eng. C* **2016**, *69*, 914.
- [92] N. Tejwan, S. K. Saha, J. Das, *Adv. Colloid Interface Sci.* **2020**, *275*, 102046.
- [93] S. N. A. Shah, M. Khan, Z. U. Rehman, *Trends Anal. Chem.* **2020**, *122*, 115722.
- [94] Z. Lin, W. Xue, H. Chen, J. Lin, *Anal. Chem.* **2011**, *83*, 8245.
- [95] S. N. A. Shah, L. Lin, Y. Zheng, D. Zhang, J. M. Lin, *Phys. Chem. Chem. Phys.* **2017**, *19*, 21604.
- [96] S. N. A. Shah, X. Dou, M. Khan, K. Uchiyama, J. M. Lin, *Talanta* **2018**, *196*, 370.
- [97] Y. Tao, M. Li, J. Ren, X. Qu, *Chem. Soc. Rev.* **2015**, *44*, 8636.
- [98] Y. Xiao, Z. Wu, Q. Yao, J. Xie, *Aggregate* **2021**, *2*, 114.
- [99] K. Zheng, J. Xie, *Trends Chem.* **2020**, *2*, 665.
- [100] K. Zheng, J. Xie, *ACS Nano* **2020**, *14*, 11533.
- [101] X. Jiang, B. Du, S. Tang, J. T. Hsieh, J. Zheng, *Angew. Chem. Int. Ed.* **2019**, *58*, 5994.
- [102] Y. Genji Srinivasulu, Q. Yao, N. Goswami, J. Xie, *Mater. Horizons* **2020**, *7*, 2596.
- [103] X. Jiang, B. Du, Y. Huang, J. Zheng, *Nano Today* **2018**, *21*, 106.
- [104] S. Ganguly, P. Das, S. Das, U. Ghorai, M. Bose, S. Ghosh, M. Mondal, A. K. Das, S. Banerjee, N. C. Das, *Colloids Surf. A Physicochem. Eng. Asp.* **2019**, *579*, 123604.
- [105] R. Wang, K. Q. Lu, Z. R. Tang, Y. J. Xu, *J. Mater. Chem. A* **2017**, *5*, 3717.
- [106] D. Tahir, S. K. Oh, H. J. Kang, S. Tougaard, *Thin Solid Films* **2016**, *616*, 425.
- [107] B. Abdullah, S. Ilyas, D. Tahir, *J. Nanomater.* **2018**, *2018*, 9823263.
- [108] H. Heryanto, B. Abdullah, D. Tahir, *J. Phys.: Conf. Ser.* **2018**, *1080*, 012007.
- [109] S. Suryani, H. Heryanto, R. Rusdaeni, A. N. Fahri, D. Tahir, *Ceram. Int.* **2020**, *46*, 18601.

**How to cite this article:** N. A. Humaera, A. N. Fahri, B. Armynah, D. Tahir, *Luminescence* **2021**, *36*(6), 1354. <https://doi.org/10.1002/bio.4084>